

Efficient coupling of inhomogeneous current spreading and electro-optical models for simulation of dynamics in broad-area semiconductor lasers

M. Radziunas*, A. Zeghuzi†, J. Fuhrmann*, Th. Koprucki*, H.-J Wünsche*†, H. Wenzel† and U. Bandelow*

*Weierstrass Institute, Mohrenstrasse 39, 10117 Berlin, Germany. Email: Mindaugas.Radziunas@wias-berlin.de

†Ferdinand-Braun-Institut, Leibniz Institut für Höchstfrequenztechnik, Gustav-Kirchhoff-Str. 4, 12489 Berlin, Germany.

Abstract—The aim of this work is an efficient implementation of a spatially resolved current spreading model defined in the vertical–lateral domain into a dynamic electro-optical solver acting in the longitudinal–lateral plane. We introduce two numerical methods for the solution of the current spreading model and perform test simulations using different approximations of the inhomogeneous current density along the active zone.

High-power edge-emitting broad-area semiconductor lasers (BALs) [Fig. 1(a)] are important light sources due to their numerous applications. Accurate modeling and simulation of BALs is critical for improving their performance or for the evaluation of novel design concepts.

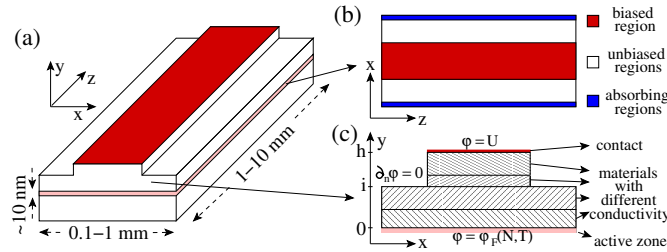


Fig. 1. Schematic representation of edge-emitting broad-area laser (a), its active zone where the TW model is defined (b), and the transverse cross-section, where the current flow equations are solved (c).

Electro-optical model: For modeling of nonlinear dynamics in BALs, we use a 2(space)+1(time) dimensional traveling wave (TW) model, see [1], [2]. In this model, we take into account only the optical field and carrier dynamics within the thin active zone of the laser along the lateral coordinates x and z , see Fig. 1(b). A set of effective model parameters represents the influence of the vertical device structure. In the computational domain, we distinguish different areas according to the positions of the contacts, trenches, or unbiased regions. The spatiotemporal dynamics of the slowly varying complex amplitudes of the counter-propagating optical fields, $E^+(z, x, t)$ and $E^-(z, x, t)$, is governed by the TW equations

$$\left[\frac{n_g}{c_0} \partial_t \pm \partial_z + \frac{i}{2\pi k_0} \partial_x^2 \right] E^\pm = -i\beta E^\pm - i\kappa E^\mp + F_{sp}^\pm, \quad (1)$$

where the propagation factor $\beta(N, E, \omega)$ depends on the local carrier density $N(z, x, t)$, includes a frequency ω dependent model for material gain dispersion, can take into account nonlinear gain compression, two-photon absorption, and the impact of heating on the gain and the refractive index. Whereas at the laser facets the optical fields satisfy reflection conditions,

at the lateral borders of the (broad enough) computational domain periodic conditions are imposed. The evolution of the carrier density $N(x, z)$ in the active zone is governed by the simple diffusive carrier rate equation

$$\partial_t N = \partial_x (D \partial_x N) + \frac{j(x, z)}{ed} - R_{sp}(N) - R_{st}(N, E, \omega). \quad (2)$$

In our previous works, the effective lateral diffusion coefficient D was assumed to be constant, and the injection current density $j(x, z)$ was set constant region-wise. For a more detailed description of the model equations and parameters, see [1], [2]. The TW model (1), (2) is the basis of the electro-optical solver BALaser [3] developed at the Weierstrass Institute.

Current spreading model: A proper description of injection and diffusion in the active zone of BALs, however, requires an adequate consideration of the current flow from the electrical contact ($y = h$) towards the active zone ($y = 0$). Since the length of the device is much larger than its width, we restrict our considerations to the study of the current flow within each transverse cross-section of the p-doped part of the device, for each fixed z_0 defined by the lateral and vertical coordinates, see Fig. 1(c). Within each of these 2-D domains at each time t_0 , we have to solve the Laplace problem

$$\nabla_{x,y} \cdot (\sigma(x, y) \nabla_{x,y} \varphi(x, y)) = 0, \quad (x, y) \in \Omega, \quad (3)$$

for the quasi-Fermi potential function $\varphi(x, y)$. The boundary conditions are given by $\varphi|_{y=h} = U$, where U is the voltage at the contact, $\varphi|_{y=0} = \varphi_{AZ}(N(x, z_0, t_0))$, where φ_{AZ} is the Fermi voltage function defined according to the Joyce-Dixon approximation of the inverse Fermi integral, and $\partial_n \varphi = 0$ at the remaining boundaries of the domain Ω . Function $\sigma(x, y)$ is the conductivity of materials within Ω . At interfaces between different materials, the continuity of the flux $\sigma \partial_n \varphi$ is preserved. The injected current entering the carrier rate eqn. (2) is defined by $j(x, z_0, t_0) = -\sigma(x, 0) \partial_y \varphi(x, 0)$. Finally, the carrier diffusion factor in the same equation can be replaced by the carrier dependent expression, $D = D(N, \partial_N \varphi_{AZ})$.

Solution of the Laplace problem: To solve the Laplace problem defined above, we apply two different approaches. The first semianalytic approach relies on a discretization of the domain Ω along the x axis into N_x equal steps, substitution of the lateral derivatives ∂_x in Eq. (3) by their finite difference analogs, and application of the method of separation of variables within the (single) lower and (one or several) upper subdomains. As a consequence, we derive a linear system of $N_x^u < N_x$ equations

$$\mathcal{M} \vec{\varphi}_i = \vec{B} \Rightarrow \vec{\varphi}_i = \mathcal{M}^{-1} \vec{B}, \quad (4)$$

for the discrete function $\vec{\varphi}_i = \varphi(x_h, i)$ at N_x^u grid points of the interface $y = i$ of upper and lower subdomains [see Fig. 1(c)] and reconstruct the semi-discrete function $\varphi(x_h, y)$ or its vertical flux $\sigma(x_h, y)\partial_y\varphi(x_h, y)$ afterwards. Here, the vector \vec{B} depends on the values of U and φ_{AZ} , whereas the matrix \mathcal{M} depends only on $\sigma(x, y)$. Thus it can be constructed and inverted in a preprocessing step. This method can be applied when all subdomains of Ω are rectangular, and the piecewise constant conductivity σ is uniform in x , $\partial_x\sigma = 0$. The second method is based on the full finite volume discretization of the whole domain. For the numerical solution of the resulting scheme, we use the software toolkit pdelib [5] developed at the Weierstrass Institute. This approach is more general, allowing various shapes of Ω and distributions of $\sigma(x, y)$. Two examples of $\varphi(x, y)$ calculated with this method are shown in Fig. 2(a) and (b). Panels (c) and (d) of the same figure show the distributions of the considered boundary function $\varphi_{AZ}(N)$ and the related $N(x)$. Blue dashed, and thin black solid curves in panels (e) and (f) represent the current density $j(x)$ calculated using the two above discussed methods. Red dashed lines in the same figure show our old piecewise constant injection approach. Note also, that in our previous modeling the total injection current $I = \iint j(x, z) dx dz$ served as a control parameter. Now this role is played by the voltage U .

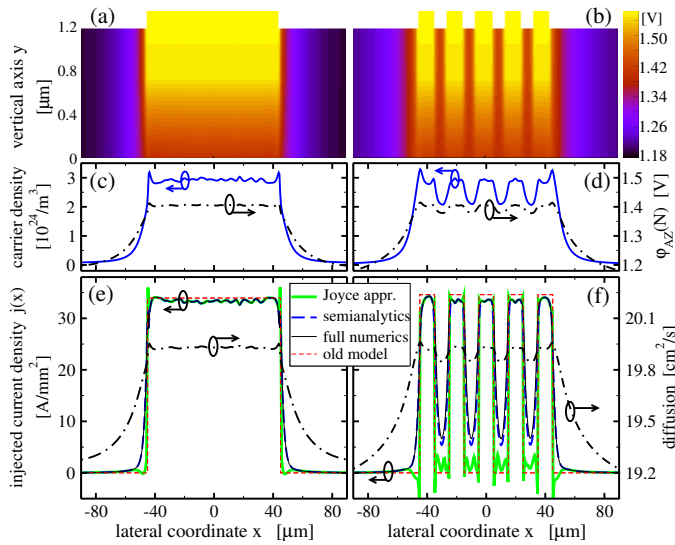


Fig. 2. Current spreading in two laser devices. (a) and (b): Fermi potential function $\varphi(x, y)$ within the domain Ω calculated for $U = 1.564 \text{ V}$ and $\varphi_{AZ}(N)$ and $N(x)$ indicated in the panels (c) and (d), respectively. (e) and (f): corresponding lateral distribution of the effective carrier diffusion D (dash-dotted) and current density $j(x)$ according to different modeling approaches.

Efficient implementation: An efficient implementation of the full (2D or even 3D) current spreading model into the electro-optical solver is related to several technical difficulties. The biggest challenge is overcoming a significant slowdown of computations, while the Laplace problem should, in general, be solved at each time instant t_0 and longitudinal position z_0 . Since for the resolution of our TW model at each (z_0, t_0) we use $\sim N_x \log(N_x)$ arithmetic operations, for the estimation of $j(x)$ at the required N_x points one should use a similar or smaller number of operations. A precomputation of \mathcal{M}^{-1} in (4) with the following recovery of the N_x^u -dimensional vector $\vec{\varphi}_i$ and N_x -dimensional vector $j(x_h)$ allows avoiding the solu-

tion of the full Laplace problem at each (z_0, t_0) . Whereas for the construction of \vec{B} and recovery of j one can exploit the FFT algorithm ($\sim N_x \log(N_x)$ operations), the matrix-vector product in Eq. (4) in general requires $\sim (N_x^u)^2$ operations which for $N_x^u \sim N_x$ computationally can be rather expensive. Similarly, one can exploit the linearity of the problem (3) together with the Green’s function approach ideas and precompute even larger matrix $\tilde{\mathcal{M}}$ such that $j(x_h) = \tilde{\mathcal{M}}\varphi_{AZ}(N(x_h))$. In this case, one avoids FFTs but needs to perform even more ($\sim (N_x)^2$) expensive matrix-vector multiplication. Fortunately, the essential elements of the matrices $\tilde{\mathcal{M}}$ and, especially, \mathcal{M}^{-1} are located around the center diagonal. Our tests have shown, that we can get a sufficient precision of $j(x_h)$ once using “cleaned” matrices M_ε obtained by cutting all matrix elements that by modulus are below some threshold $\theta_\varepsilon = \varepsilon \cdot \max(|M_{ij}|)$. Typically, depending on ε , such cleaned matrices have only 10-20 non-vanishing diagonals, allowing to avoid the curse of a too expensive matrix-vector multiplication.

Another computationally much cheaper approach requiring only $\sim N_x$ arithmetic operations exploits the Joyce approximation of the solution of the Laplace problem [4]. According to this method, the injection density $j(x)$ is proportional to $U - \varphi_F(x)$ just below the electrical contact, and to $\partial_x^2 \varphi_F(x)$ outside the contact, see thick green curves in Figs. 2(c) and (d). Since the main weakness of this approach is at the edges of the contact, it can be useful when the contact is broad but fails to provide reliable results when there are several narrow contacts located close to each other.

The semianalytic method with the additional cleaning of the matrix \mathcal{M}^{-1} and the Joyce approximation method as well as the laterally distributed carrier diffusion model were implemented into the electro-optical solver BALaser [3]. Test simulations of the extended TW model (1), (2) over one ns on a multi-core computer using ten processes have shown the following performance results. The simulations of the BAL using the old model with the piecewise constant j and constant D took 541 s. After inclusion of the distributed D , the simulation time was 556 s. After an additional inclusion of the Joyce approximation of j , this time was 568 s. The usage of a more precise j obtained by solving the Laplace problem with the matrix cleaning threshold of 10^{-3} and 10^{-7} was slowing down the simulations to 634 s and 639 s, respectively.

In conclusion, we have discussed an efficient implementation of the current spreading model into the electro-optical solver. The speed of calculations was reduced only by $\sim 15\%$.

ACKNOWLEDGMENT

This work is supported by the German Federal Ministry of Education and Research contract 13N14005 as part of the EffiLAS/HotLas project.

REFERENCES

- [1] M. Radziunas and R. Čiegis, *Math. Model. and Anal.*, 19:627-644, 2014
- [2] M. Spreemann et al., *IEEE J. of Quantum Electronics*, 45:609-616, 2009
- [3] BALaser: A software tool for simulation of dynamics in broad area semiconductor lasers. <http://www.wias-berlin.de/software/balaser/>
- [4] W.B. Joyce, *J. of Appl. Physics*, 53:7235-7239, 1982
- [5] pdelib: a finite volume and finite element toolbox for PDEs. <http://www.wias-berlin.de/software/pdelib/>